Oxide-ion Conductivity in $Cu_xCe_{1-x}O_{2-\delta}$ ($0 \leq x \leq 0.10$)

Arup Gayen[a], K. R. Priolkar[b], A. K. Shukla[a], N. Ravishankar[c], M. S. Hegde[a, *]

[a] *Solid State and Structural Chemistry Unit, Indian Institute of Science, Bangalore-560012, India*

[b] *Department of Physics, Goa University, Taleigao Plateau, Goa-403206, India*

[c] *Materials Research Centre, Indian Institute of Science, Bangalore-560012, India*

∗ To whom correspondence should be addressed

E-mail: mshegde@sscu.iisc.ernet.in (M. S. Hegde)

Fax: +91-80-2360-1310

Abstract

Up to 10 atom % of copper readily substitutes for cerium in ceria. It is found that at oxygen partial pressures between 0.21 atm and 10^{-5} atm, $Cu_xCe_{1-x}O_{2-\delta}$ ($0 \leq x \leq 0.10$) solid solution behave as an oxide-ion electrolyte. Interestingly, $Cu_{0.10}Ce_{0.90}O_{2-\delta}$ exhibits the oxide-ion conductivity of *ca.* 10^{-4} $ohm^{-1}cm^{-1}$ at 600 ^oC at an oxygen partial pressure of 10^{-5} atm.

Keywords: A. Oxides; B. Chemical synthesis; C. Impedance spectroscopy; D. Defects; D. Ionic conductivity

1. Introduction

In the literature [1-10], a majority of activity in the study of oxide-ion electrolytes has centred on oxides that crystallize in the fluorite structure and related compounds obtained by addition of suitable dopants. Among these, ceria-based oxide-ion electrolytes are more readily reducible and hence exhibit an electronic conductivity component at low partial pressures of oxygen. One of the best oxide-ion electrolyte is $(CeO_2)_{0.8}(Sm_2O_3)_{0.2}$, which has a conductivity value of about 0.3 $ohm^{-1}cm^{-1}$ at 1273 K and an activation energy of 0.83 eV [11]. Mixed oxide samples of CuO and CeO_2 have also been studied by Knauth et al. [12] with a motive to determine the thermodynamic activities of copper oxide in mixed nanostructural CeO_2. In another study, Ni anode with yttria-stabilized zirconia (YSZ) in a solid oxide fuel cell has been replaced with 40 wt.% Cu and 20 wt.% CeO_2 held in place by YSZ electrolyte so as to circumvent the problem of carbon formation on the Ni anode [13]. This is because Cu is an excellent electronic conductor while CeO_2 has high catalytic activity for hydrocarbon oxidation [14].

In this paper, we report the oxide-ion conductivity in $Cu_xCe_{1-x}O_{2-\delta}$ ($0 \leq x \leq 0.10$) solid solution since such a study is lacking in the literature. It is found that at oxygen partial pressures (pO_2) between 0.21 atm and 10^{-5} atm, $Cu_xCe_{1-x}O_{2-\delta}$ ($0 \leq x \leq 0.10$) solid solution behave as pure oxide-ion electrolytes, and the oxide-ion conductivity of $Cu_{0.10}Ce_{0.90}O_{2-\delta}$ at 600 ^oC under $pO_2 \sim 10^{-5}$ atm is about 10^{-4} $ohm^{-1}cm^{-1}$. We have also found copper-substituted ceria to be an excellent oxidation/reduction catalyst [15] and it could as well be that copper-substituted ceria may help circumventing carbon formation in the solid oxide fuel cells in a manner akin to that reported by Park et al. [13].

2. Experimental

2.1. Synthesis of ceria and copper-ceria solid solutions

CeO_2 and $Cu_xCe_{1-x}O_{2-\delta}$ ($0 \leq x \leq 0.10$) solid solution were prepared by solution-combustion route. The combustion was carried out in an open furnace placed in a fuming cupboard fitted with an exhaust. The combustion mixture for the preparation of 5 atom % Cu-substituted CeO_2 comprised $Ce(NO_3)_3.6H_2O$, $Cu(NO_3)_2.3H_2O$ and $C_2H_6N_4O_2$ (oxalyldihydrazide) in the molar ratio 0.95 : 0.05 : 1.475. Oxalyldihydrazide (ODH) prepared from diethyl oxalate and hydrazine hydrate was used as the fuel. In a typical preparation, 10 g of $Ce(NO_3)_3.6H_2O$ (Rolex Chemical Industries, 99.9%), 0.293 g of $Cu(NO_3)_2.3H_2O$ (S. D. Fine-Chem. Ltd., 99.9%) and 4.227 g of ODH were dissolved in 50 ml of distilled water in a beaker of 2 litre capacity. The excess water was then evaporated and the redox mixture was placed in an open furnace maintained at ~350 ^oC; the reaction mixture was partially covered with a lid for the free liberation of gases. Initially, the solution boiled with frothing and foaming followed by complete dehydration when the surface ignited, burning with a flame (~1000 ^oC), and yielding a voluminous solid product within 5 minutes. The product, deposited throughout the inner walls and the lid, was wiped out into a borosilicate dish, covered with a watch glass, and introduced into a muffle furnace at 500 ^oC for about 30 min to remove any residual volatile matter. Pure CeO_2 and 10 atom % Cu-substituted CeO_2 were prepared in a similar manner.

2.2. Characterization

The samples were characterized by X-ray diffraction (XRD) using a Philips X'Pert diffractometer at a scan rate of 0.5^o min^{-1} with 0.02^o step size in the 2θ range 20^o to 80^o. The structural refinement was done using the FullProf–fp2k program. The X-ray line broadening (Scherrer formula) indicated the samples to be nano-sized crystallites with average diameter of 15 nm. TEM studies of ceria and copper-substituted ceria samples were carried out using a JEOL JEM-200CX transmission electron microscope operated at 200 kV.

2.3. Conductivity measurement

For electrical conductivity measurements, the as-prepared samples were cold pressed by applying a pressure of 1.5 ton and heated at 600 ^oC for 6 hours to obtain disc shaped samples of 8 mm diameter and ~ 1 mm thickness. The sintered pellets were coated with gold paste A-3360 and impedance spectra were obtained using Hewlett Packard 4194-A Impedance Gain Phase Analyzer. A two-probe conductivity cell was used for impedance measurements. Measurements were conducted in oxygen, air, 5% oxygen in helium, nitrogen and argon to achieve a range of oxygen partial pressures between 1 and 10^{-5} atm. The ultra high pure (UHP) gases were obtained from Bhuruka Gases Ltd., Bangalore. Prior to each electrical measurement, the sample was held at a desired temperature for *ca*. 30 minutes for equilibrating. The data were collected in the temperature range between 250 ^oC and 600 ^oC.

3. Results and Discussion

3.1. Structural studies

The observed, calculated and difference powder XRD patterns for CeO_2, $Cu_{0.05}Ce_{0.95}O_{2-\delta}$, and $Cu_{0.10}Ce_{0.90}O_{2-\delta}$ are shown in Fig. 1(a)-(c), respectively. All the diffraction lines could be indexed to the fluorite structure of ceria. The patterns have been Rietveld refined by simultaneously varying 19 parameters, which include overall scale factor, background parameters, unit cell, half width, shape and isotropic thermal parameters along with oxygen occupancy. As can be seen the fits are quite good. The R_{Bragg}, R_F and R_P values for CeO_2 are 1.54, 0.977, and 6.66% respectively and the cell parameter for the same is 5.414 (1) Å. Total oxygen in CeO_2 is 1.88 (3). The refined parameters R_{Bragg}, R_F and R_P, the lattice parameter 'a' and oxygen occupancy for $Cu_xCe_{1-x}O_{2-\delta}$ samples have been listed in Table 1 along with those of CeO_2. Clearly Cu^{2+} ions are substituted for Ce^{4+} ions and accordingly, there is an increase in the oxygen vacancy with the increase in Cu^{2+} ion substitution. Ionic radius of Cu^{2+} is 0.73 Å and that of Ce^{4+} is 0.97 Å. Thus, a large decrease in the lattice parameter is expected on Cu^{2+} ion substitution in the CeO_2 lattice. But, simultaneous increase in the oxide ion vacancy leads to an increase in the lattice parameter. Therefore, only a small decrease in 'a' is observed. Average crystallite size of CeO_2 calculated from the Scherrer method is ~15 nm, which is in agreement with the transmission electron micrograph of as-prepared samples shown in Fig. 2(a). Fig. 2(b) shows the TEM image of 5 atom % Cu substituted CeO_2. Copper oxide particles on the crystallite surfaces could not be detected. The ring type diffraction pattern (not shown) can be indexed only to polycrystalline CeO_2 in the fluorite structure and CuO diffraction

rings have not been observed in the pattern. No peaks corresponding to either copper metal or oxides of copper are seen in the XRD patterns. This indicates that up to 10 atom % of Cu^{2+} can be substituted for cerium ions in CeO_2 in case of samples prepared by solution-combustion route. In an earlier study, we had shown by XRD, XPS and EXAFS studies that in $Ce_{1-x}Cu_xO_{2-\delta}$ prepared by employing ceric ammonium nitrate as the cerium precursor and ODH as the fuel, Cu^{2+} ion substitutes for Ce^{4+} in CeO_2 [16]. It was also shown that oxide-ion vacancies are present around Cu^{2+}-ion. With ceric ammonium nitrate as precursor, sizes of $Ce_{1-x}Cu_xO_{2-\delta}$ crystallites were ~35 nm, and only up to 7 atom % of Cu^{2+}-ions could be substituted. By contrast, cerrous nitrate used here gives smaller crystallites (~15 nm) and an increased solid solubility of Cu^{2+}-ions even up to 13 atom %. The $Cu_xCe_{1-x}O_{2-\delta}$ samples were sintered at 600 ^oC, the highest temperature at which conductivity measurement was carried out. The XRD patterns, magnified by 15 times with respect to CeO_2 (111) peak, of the sintered samples did not show any Bragg peak due to CuO phase in the 2θ range of 35^o to 45^o as can be seen from the Fig. 3. Thus, there seems to be no grain boundary separation of CuO phase. However, there is growth in the particle size from 15 nm to 20-25 nm upon sintering. TEM recorded on crushed powder of these sintered pellets (Fig. 4) clearly show that the particle sizes are still in the nano region, with average crystallite size of about ~ 25 nm in agreement with the XRD studies on these samples (Fig. 3). The diffraction ring patterns (not shown) also did not show lines due to CuO. Thus annealing up to 600 ^0C, although results in the growth of crystallites from 15 nm to 25 nm, does not lead to any impurity phase segregation at the grain boundaries. We have studied ionic conductivity of pure CeO_2 and two compositions of copper-substituted ceria, $Cu_xCe_{1-x}O_{2-\delta}$, namely x = 0.05 and 0.10.

3.2. Conductivity studies

The impedance spectra at 600 ^{o}C in oxygen for pure, 5 atom % and 10 atom % Cu-substituted CeO_2 are presented in Fig. 5. These spectra show a single arc, which may be due to two closely overlapping semicircles [17]. The high-frequency component may include contributions from the bulk as well as from parallel conduction along grain boundaries. The lower frequency component represents conventional blocking by grain boundaries oriented largely normal to the current. It is clearly seen that copper substitution increases the bulk conductivity of the sample. Interestingly, the data in Fig. 5 show a monotonic decrease in the grain boundary resistance from about 4×10^4 ohm in CeO_2 to about 3.3×10^2 ohm for 10 atom % copper-substituted CeO_2. It is noteworthy that the grain boundary resistance depends on impurity segregation, which decreases for nano particles owing to increased boundary area as reflected in the transmission electron micrographs of the pure CeO_2 and copper-substituted ceria sample. Activation energy obtained from measurements over a range of temperature from 300 ^{o}C to 600 ^{o}C (Fig. 6) for pure CeO_2 is about 0.90 eV, while it is found to be 0.67 eV in the case of 10 atom % Cu-substituted sample. Near-parallel lines in the Arrhenius plots (Fig. 6) for pure CeO_2, and Cu-substituted CeO_2 samples suggest that conductivity increase is due to extrinsic defects created by substitution of Cu^{2+}-ions for cerium ions in CeO_2.

In order to see the effect of oxygen partial pressure (pO_2) on the conductivity behaviour of these materials, measurements have been carried out at five different values of pO_2 and the data for pure CeO_2, and 5 atom % and 10 atom % Cu-substituted CeO_2 samples are presented in Fig. 7(a) and 7(b), respectively. At high pO_2 (>0.21 atm), the conductivity of copper-substituted CeO_2 samples increases with

pO_2 (Fig. 7(b)), which can be accounted in the light of the following defect equilibrium,

$$O_2(g) + Ce_{Ce} \rightarrow CeO_2 + \frac{1}{4}V_{Ce}^{''''} + \frac{1}{3}V_{Ce}^{'''} + 2h^{\bullet} \qquad (1)$$

resulting in, $$h = k_1 p_{O_2}^{1/2} \qquad (2)$$

Accordingly, at high values of oxygen partial pressures, electron-hole conduction becomes important, and the slope of log σ vs log pO_2 plot is 1/2. But, at pO_2 values in the range 0.21 atm to 10^{-5} atm, the conductivity exhibits a pO_2-independent behaviour showing pure electrolytic oxide-ion conduction in the Cu-substituted CeO_2 samples. By contrast, in the case of pure CeO_2, the conductivity continuously increases with decreasing pO_2 values (Fig. 7(a)) suggesting primarily electronic conduction, which is in accordance with the findings of Fujimoto and Tuller [18].

4. Conclusions

The oxygen partial pressure dependence of the conductivity in copper substituted CeO_2 has been studied between 250 ^{o}C and 600 ^{o}C. It is found that the conductivity is nearly independent of the oxygen partial pressure in the range 0.21–10^{-5} atm. These data suggest copper-substituted ceria to be pure oxide-ion electrolytes, under these conditions.

Acknowledgements

A. Gayen is thankful to the Council of Scientific and Industrial Research, Government of India, New Delhi for the award of a Research Fellowship. K. R. Priolkar thanks Indian Academy of Sciences for a Summer Research Fellowship. Financial support from the Department of Science and Technology, Government of India, New Delhi is gratefully acknowledged.

References

[1] B.C.H. Steele, in: High Conductivity Solid Ionic Conductors, ed. T. Takahashi, World Scientific, Singapore, 1989.

[2] J.A. Kilner, B.C.H. Steele, in: Nonstoichiometric Oxides, ed. O.T. Sorenson Academic Press, New York, 1981.

[3] R.M. Dell, A. Hooper, in: Solid Electrolytes, eds. P. Hagenmuller and W. Van Gool, Academic Press, New York, 1978, p. 291.

[4] H. Inaba, H. Tagawa, Solid State Ionics 83 (1996) 1.

[5] H.L. Tuller, Solid State Ionics 131 (2000) 143.

[6] B. Cales, J.F. Baumard, J. Phys. Chem. Solids 45 (1984) 929.

[7] S. Dickmen, P. Shuk, M. Greenblatt, Solid State Ionics 126 (1999) 89.

[8] Y. Gu, G. Li, G. Meng, D. Peng, Mat. Res. Bull. 35 (2000) 297.

[9] T. Mori, J. Drennan, Y. Wang, J.H. Lee, J.G. Li, T. Ikegami, J. Electrochem. Soc. 150 (2003) A665.

[10] R. Gerhardt-Anderson, A.S. Nowick, Solid State Ionics 5 (1981) 547.

[11] R.T. Dirstine, R.N. Blumenthal, T.F. Kuech, J. Electrochem Soc. 126 (1979) 264.

[12] P. Knauth, G. Schwitzgebel, A. Tschöpe, S. Villain, J. Solid State Chem. 140 (1998) 295.

[13] S. Park, J.M. Vohs, R.J. Gorte, Nature 404 (2000) 265.

[14] A. Trovarelli, Catal. Rev. Sci. Eng. 38 (1996) 439.

[15] P. Bera, S.T. Aruna, K.C. Patil, M.S. Hegde, J. Catal. 186 (1999) 36.

[16] P. Bera, K.R. Priolkar, P.R. Sarode, M.S. Hegde, S. Emura, R. Kumashiro, N.P. Lalla, Chem. Mater. 14 (2002) 3591.

[17] Y.M. Chiang, E.B. Lavik, I. Kosacki, H.L. Tuller, J.Y. Ying, J. Electroceramics 1 (1997) 7.

[18] F.H. Fujimoto, H.L. Tuller, in: Fast Ion Transport in Solids, Proc. Int. Conf. Lake Geneva, P. Vashishta, J.N. Mundy and G.K. Shenoy eds. (North Holland, Amsterdam, 1979) p.649.

Figure Captions

Fig. 1. Rietveld refined powder XRD patterns for (a) CeO_2, (b) $Cu_{0.05}Ce_{0.95}O_{2-\delta}$ and (c) $Cu_{0.10}Ce_{0.90}O_{2-\delta}$.

Fig. 2. TEM image of as-prepared (a) CeO_2, (b) 5 atom % copper-substituted CeO_2.

Fig. 3. XRD patterns of (a) CeO_2, (b) $Cu_{0.05}Ce_{0.95}O_{2-\delta}$ and (c) $Cu_{0.10}Ce_{0.90}O_{2-\delta}$ samples sintered at 600 ^oC for 10 h.

Fig. 4. TEM images of crushed powders of the pellets of (a) CeO_2, and (b) $Cu_{0.05}Ce_{0.95}O_{2-\delta}$ samples sintered at 600 ^oC for 10 h.

Fig. 5. Typical impedance spectra for (a) CeO_2, (b) $Cu_{0.05}Ce_{0.95}O_{2-\delta}$ and (c) $Cu_{0.10}Ce_{0.90}O_{2-\delta}$ at 600 ^oC at pO_2 of 1 atm along with the fitted curves (solid lines).

Fig. 6. log σ versus 1000/T plots for (a) CeO_2, (b) $Cu_{0.05}Ce_{0.95}O_{2-\delta}$ and (c) $Cu_{0.10}Ce_{0.90}O_{2-\delta}$ in the temperature range 250 ^oC to 600 ^oC in air.

Fig. 7. log σ versus log pO_2 plots at 600 ^oC for (a) CeO_2, and (b) copper-substituted ceria.

Table 1

Rietveld refined parameters of CeO_2 and $Cu_xCe_{1-x}O_{2-\delta}$ crystallites.

Sample	a (Å)	R_{Bragg}	R_F	R_P	Oxygen Occ.
CeO_2	5.414 (1)	1.54	0.977	6.66	1.88 (3)
$Cu_{0.05}Ce_{0.95}O_{2-\delta}$	5.4117 (8)	1.39	1.12	6.71	1.84 (3)
$Cu_{0.10}Ce_{0.90}O_{2-\delta}$	5.414 (1)	1.71	1.41	6.90	1.77 (3)

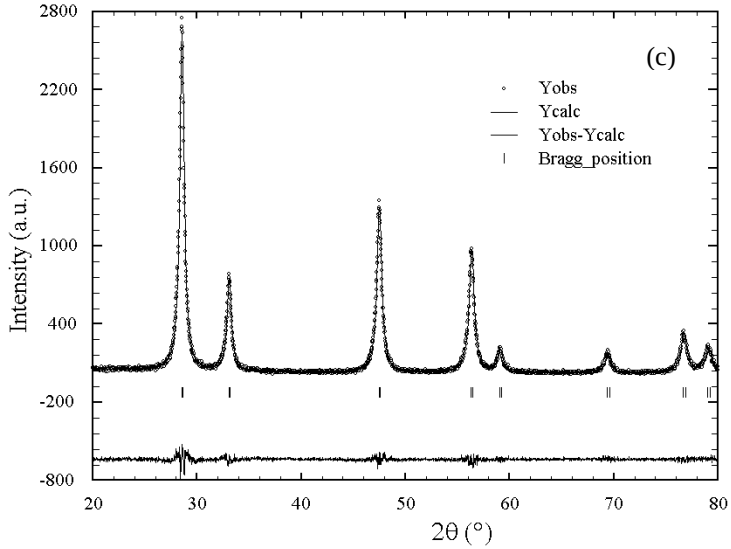

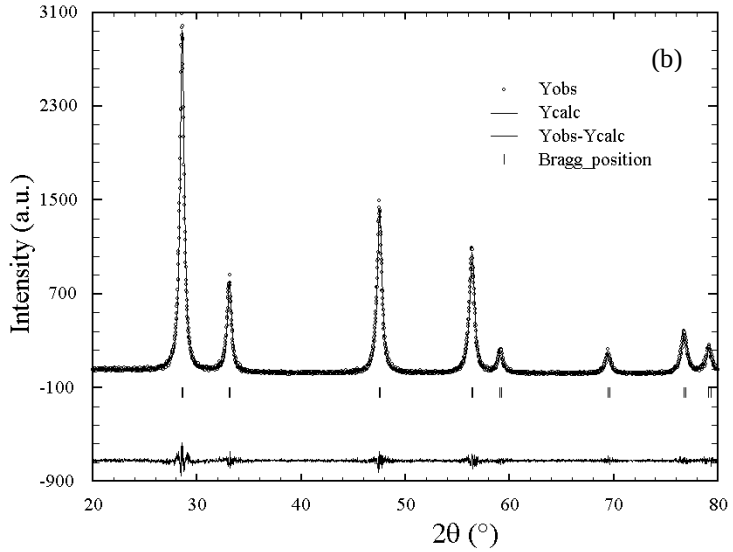

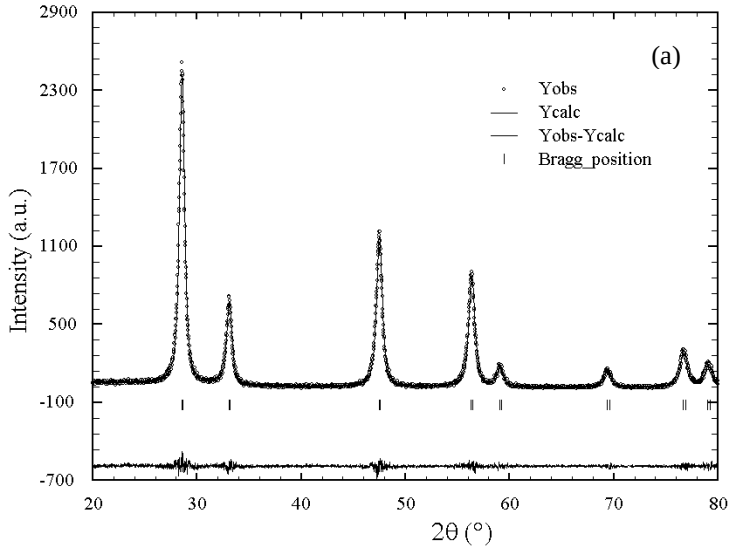

Fig. 1. Gayen et al.

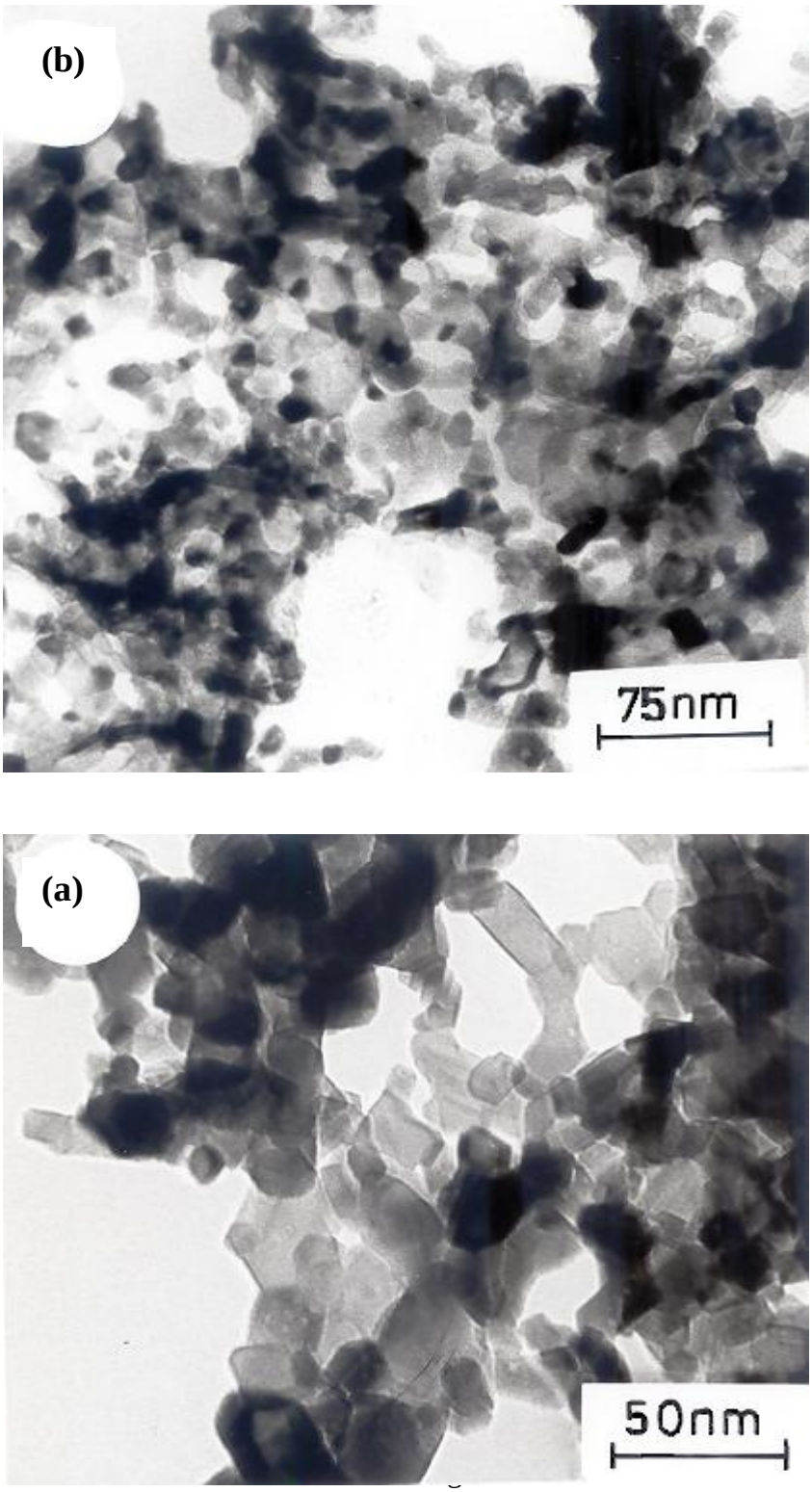

Fig. 2. Gayen et al.

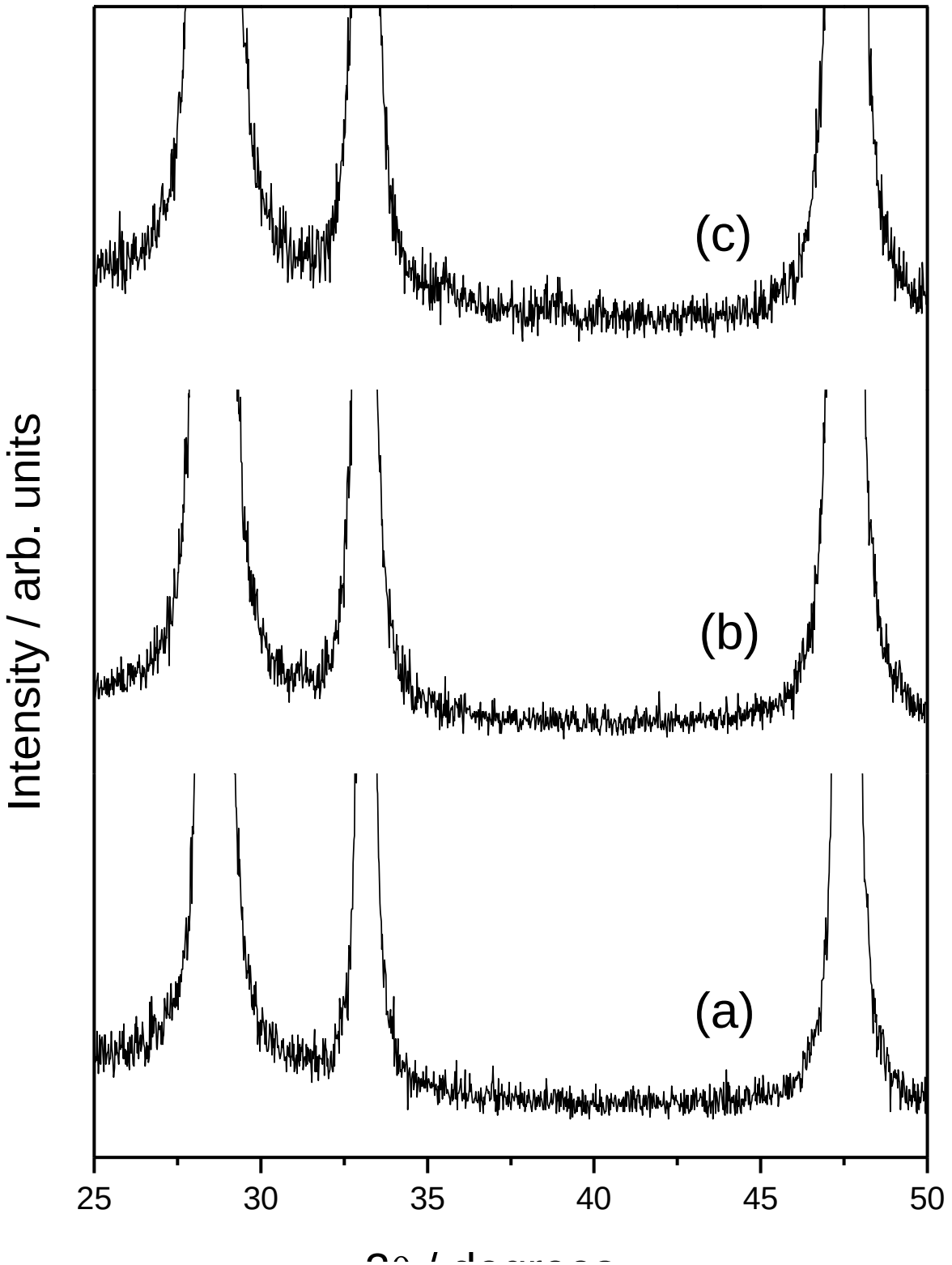

Fig. 3. Gayen et al.

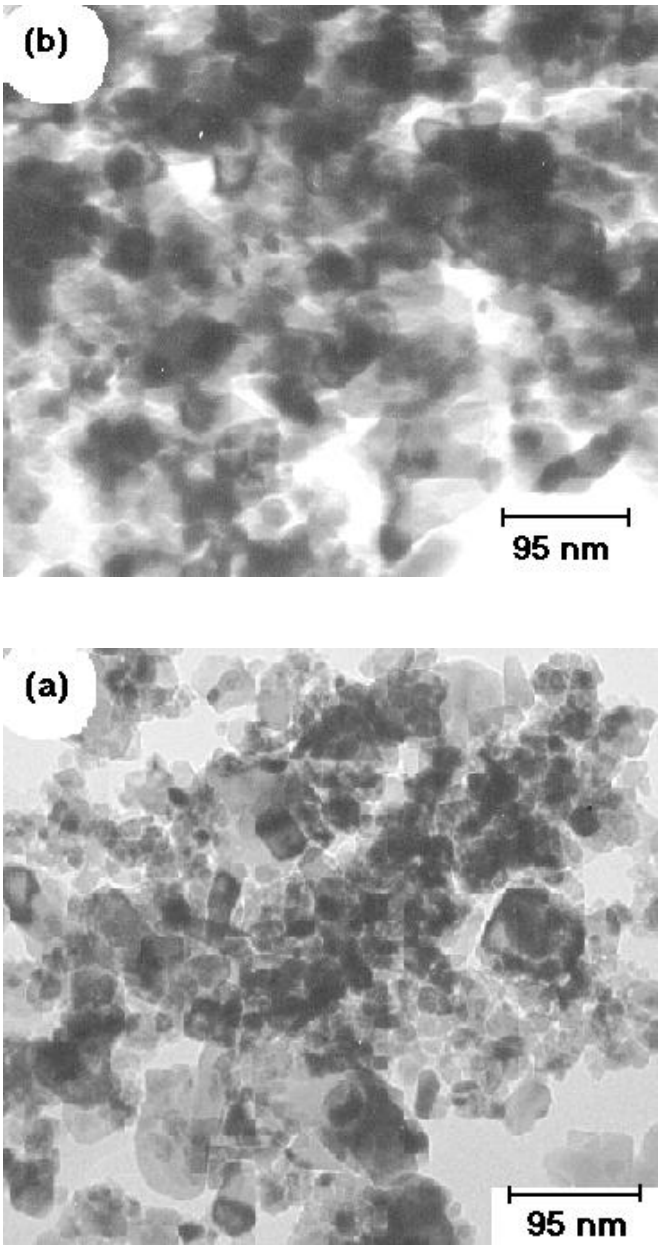

Fig. 4. Gayen et al.

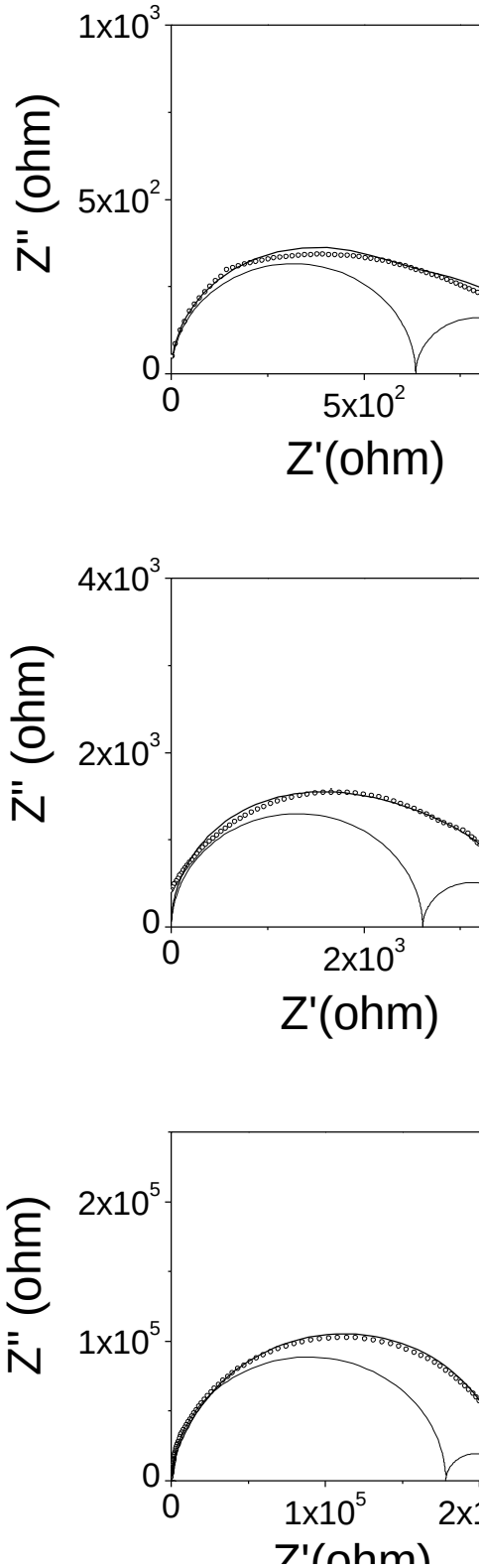

Fig. 5. Gayen et al.

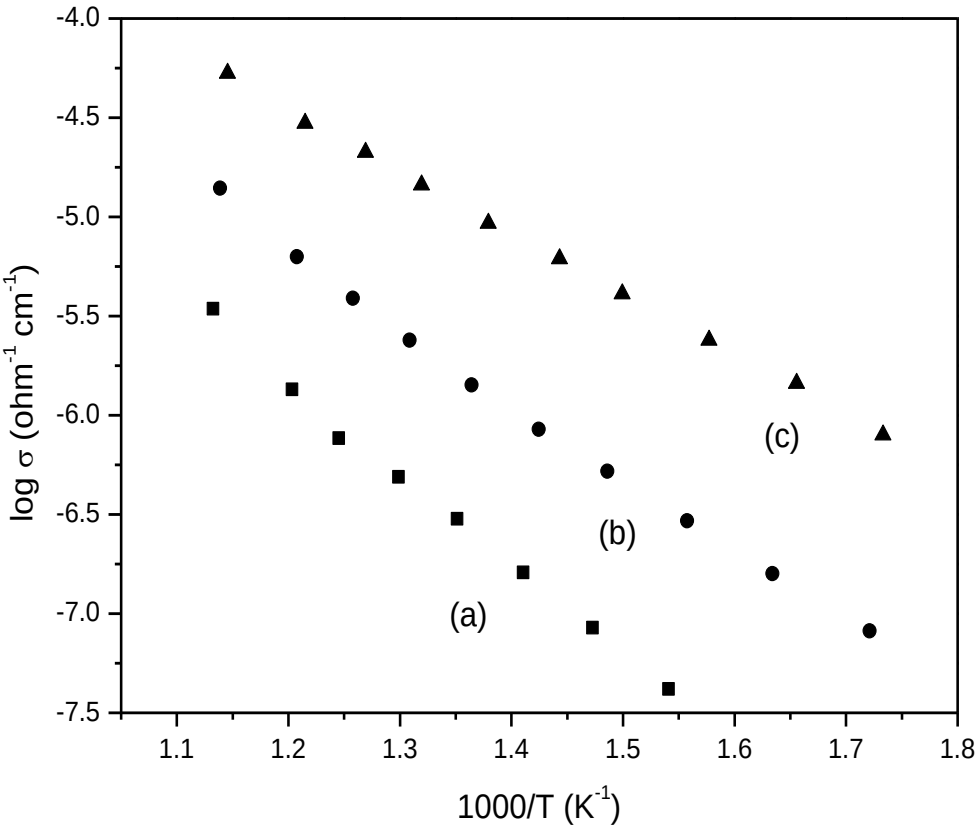

Fig. 6. Gayen et al.

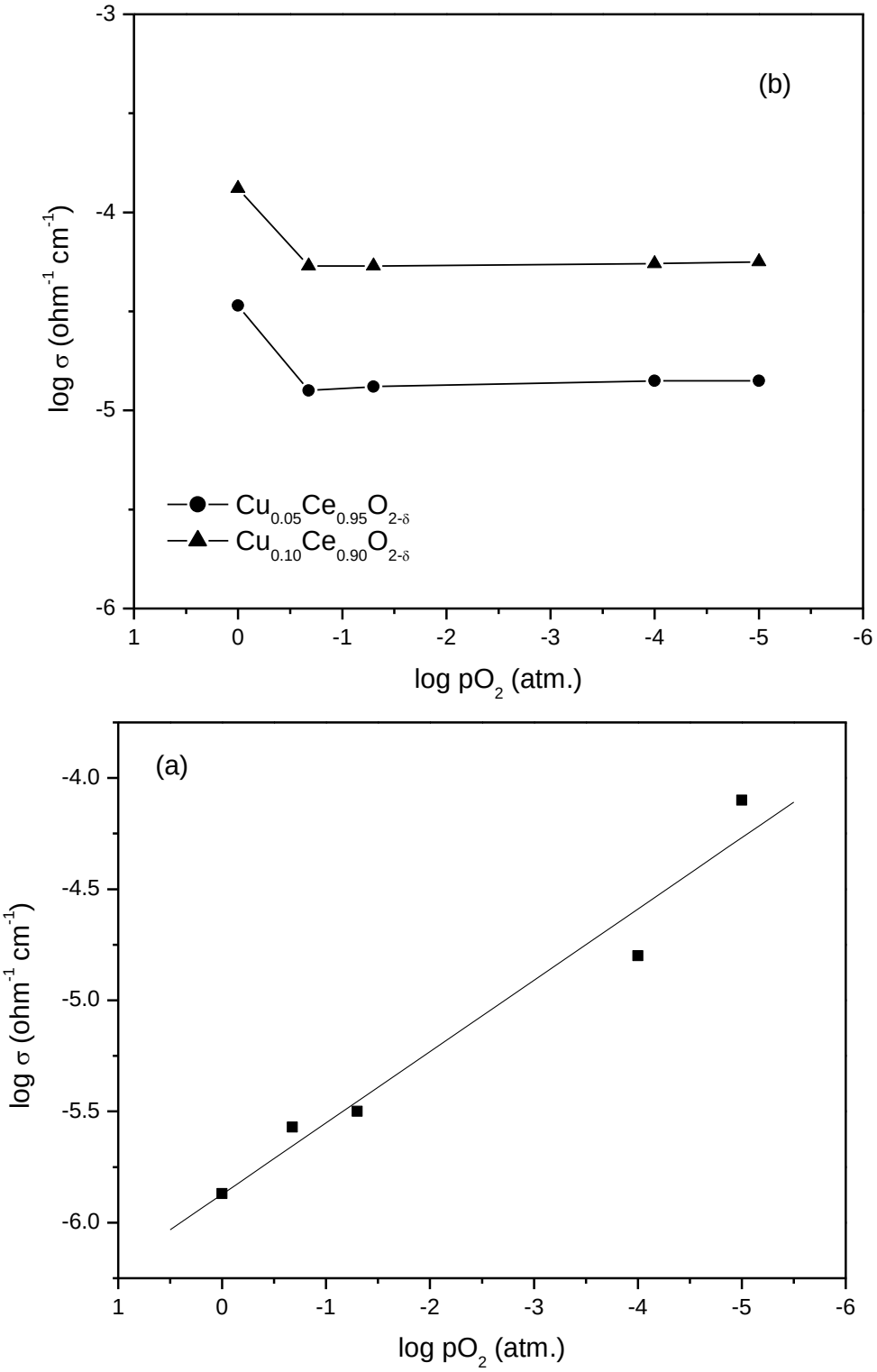

Fig. 7. Gayen et al.